

# The Effect of Propeller Pitch on Ship Propulsion

Deniz Ozturk<sup>a</sup>, Cihad Delen<sup>a</sup>, Samir E. Belhenniche<sup>b</sup>, Omer Kemal Kinaci<sup>a</sup>

The appropriate choice of a marine engine identified by using self-propulsion model tests is compulsory, in particular with respect to the improvement of vessel performances. Numerical simulations or experimental methods provide insight into the problem of flow, where fixed pitch propellers or controllable pitch propellers are preferred. While calculation methods are time consuming and computationally demanding for both propeller types, hydrodynamic performance assessment has more workload in controllable pitch propellers. This paper aims to describe and demonstrate the practicability and effectiveness of the self-propulsion estimation (SPE) method in understanding the effect of propeller pitch on ship propulsion. Technically, the hydrostatic and geometric characteristics of the vessel and open-water propeller performances are the focal aspects that affect the self-propulsion parameters estimated by the SPE method.

## KEY WORDS

- ~ Controllable pitch
- ~ Fixed pitch
- ~ CPP
- ~ Self-propulsion estimation method
- ~ KCS
- ~ DTC

a. Istanbul Technical University, Faculty of Naval Architecture and Ocean Engineering, Istanbul, Turkey

e-mail:kinacio@itu.edu.tr

b. University of Science and Technology - Mohamed Boudiaf, Marine Engineering Department, Oran, Algeria

doi: 10.7225/toms.v11.n01.w09

This work is licensed under 

Received on: Aug 1, 2021 / Revised on: Nov 28, 2021 / Accepted on: Jan 27, 2022 / Published online: Feb 19, 2022

The input coefficients for SPE have been identified using a code that generates propeller open-water performance curves. The propellers utilized to study pitch variations have been based on the Wageningen B-series propeller database. The method was first validated on the full size Seiun Maru ship whose sea trial tests are available in literature. After extensive calculations for full size KCS and DTC at service speeds, the study focused on the effect of the Froude number on propulsion parameters. These calculations have demonstrated that greater propeller pitch does not improve propulsion efficiency, and that maximum propeller efficiency changes with a ship's forward speed.

## 1. INTRODUCTION

Ship propulsion systems and auxiliary power engines are a major investment for the owner or operator. Therefore, all the factors that contribute to the total cost of marine engines should be examined, while still bearing in mind the vessel's performance. Vessel performance can be enhanced on different navigation routes and in different operating conditions by integrating suitable propeller systems; Controllable pitch propellers (CPP) are offered as an alternative, especially for ships in inland waters. Inland waterway vessels change speed more frequently than oceangoing ships, causing the main engine to overload during navigation. CPP modifies ship speed through propeller pitch adjustment, instead of by changing the rotational speed of the main engine, as is the case with fixed-pitch propellers (FPP).

Some studies on the optimization of Wageningen B-series propeller design, aiming to state or improve the performance of marine propulsion systems, have been conducted. Benini (2003) focused on achieving the maximum efficiency and thrust coefficient for B-series propellers through multi-objective design optimization steps. The author established that the best screw

configuration for a given thrust coefficient can be obtained. Another design optimization research was presented by (Gaafary et al., 2011), who chose a widely used B-series propeller. Cavitation, material strength and propeller thrust constraints were formulated to reach the optimum point practically at the open water diagram. An open-source propeller optimization code was developed by Epps et al. (2009) who changed rotation rate to explain its effects on motor sizing. Cavitation restrictions have also been considered and efforts made to develop a code based on a precise and influential propeller and axial flow turbine design tool. A practical procedure was developed to select the optimum propeller by considering minimum fuel consumption (Tadros et al., 2021, 2020a). The model helps select a high-efficiency B-series FPP through power requirement prediction. The authors also applied a similar optimization approach to a fishing trawler to obtain the conceptual design (Tadros et al., 2020b). Several components were considered in the simulation model, such as the injection system, turbocharger, intercooler, intake and exhaust manifolds, engine cylinders and atmospheric initial conditions.

The literature on CPPs mainly focuses on open-water use of the well-known Wageningen B-series propellers. The B-series propeller database consists of FPPs and has been used quite frequently due to the lack of systematic data on CPPs. In spite of several experimental studies conducted, recent studies on CPPs are generally based on computational fluid dynamics (CFD) methods. Caldas et al. (2010) carried out CFD simulations for ducted propellers in open water conditions, at a specific propeller pitch ratio (P/D) and different nozzle geometries. The comparison with experimental data showed that the Reynolds-averaged Navier-Stokes (RANS) models were capable of predicting propulsive factors. Heinke (2011) conducted open-water tests, cavitation tests, and laser doppler velocimetry (LDV) measurements for a skewed CPP to study the influence of hub and gap forces in open-water. The influence of pitch was not studied, and the number of revolutions, varying between 15, 20 and 25 rps, had little effect on open water characteristics. Dang et al. (2012) looked into propeller thrust, torque on the shaft and blade spindle torque on Wageningen C- and D-series propellers by applying experimental fluid dynamics (EFD) and CFD. The authors stated that a quasi-steady open-water test technique was found to be reliable and dramatically reduced tank testing time. Xiong et al. (2013) showed that the open-water efficiency of CPPs was sensitive to boss cap fins depending on the forward velocity changes. Numerical simulations with and without boss cap fins were performed, taking into consideration airfoil profile, axial position, and circumferential angle. Maritime Research Institute Netherlands (MARIN) launched the Joint Industry Project in 2011 to create Wageningen C- and D-series for both open and ducted CPPs (Dang et al., 2013). In this extensive study conducted using

a wide range of pitch ratios, C-Series propellers were found to be more efficient.

Research on ship self-propulsion and prediction methods has picked up pace in the decades that followed the widespread use of supercomputers. Ship self-propulsion and course-keeping can be simulated by CFD-based methods, using the current state of the art technology. As explained in detail by Farkas et al. (2018), an extensive numerical and experimental study was conducted to predict ship self-propulsion point by using several extrapolation methods. Jasak et al. (2019) studied general flow characteristics and propeller-hull interactions, comparing sea trial measurements and full size numerical results. Recent numerical simulations utilize RANS-based CFD (Sezen et al., 2018; Bakica et al., 2019) to obtain self-propulsion parameters. Using the same tool, Carrica et al. (2010) studied the issue of self-propulsion of a generic submarine near the surface. The details of interaction with the surface were examined in simulations carried out both in calm and heavy seas. Some other studies aimed to improve estimation methodologies, such as the use of the coupled BEM/RANSE approach (Gaggero et al.; 2017) or the use of actuator disk models (Villa et al.; 2019). The self-propulsion estimation (SPE) method only makes use of the hydrostatic and geometric properties of the ship and open-water propeller performance (Kinaci et al.; 2018), (Kinaci et al.; 2020). The SPE method is a highly practical and cost-effective ship propulsion performance assessment tool, in contrast to numerical computations or self-propulsion experiments.

CPP is preferable for cutting down fuel consumption (Makino et al.; 2017), when load protection is properly controlled (Ji et al.; 2018) to prevent propeller blade deformation. However, the hydrodynamic assessment of CPP in the preliminary ship design stage is more complex than that of FPP. The hydrodynamic performance of the propeller, predicted using open-water tests, varies with propeller pitch modification. In case of FPP, the tests need to be conducted only once, whereas they have to be repeated multiple times to cover the entire range of CPP propeller pitches. Although the amount of work required to assess the self-propulsion of a ship with a traditional FPP (bare hull resistance tests, open-water propeller tests, self-propulsion tests, etc.) is extensive, workload necessary to estimate the hydrodynamic performance of a CPP is far greater. In addition, whenever a propeller positioned behind the ship changes its mode of operation, it simultaneously changes the hull-propeller interaction. Therefore, open-water propeller test alone is insufficient to study CPP performance and behind-the-hull cases should also be researched. Various researchers have attempted to incorporate the effects of the hull-CPP interaction, such as Martelli et al. (2014), who took into account the effect of the yaw motion of the ship during maneuvering on the ability to properly control CPP. However, the studies are very limited and generally

look at CPPs from a control engineering perspective. From the marine engineering perspective, the effects of CPPs on surge motion, which the ships are subjected to most of the time, (and accordingly on self-propulsion characteristics) are required. This study proposes a fast and practical method of overcoming the challenges encountered during estimation - the adoption of a practical self-propulsion estimation method recently published in literature (Kinaci et al.; 2020).

As mentioned above, the effect of propeller pitch can not be understood by using a single fixed pitch propeller. The establishment of the effect of pitch on ship self-propulsion requires parametric studies where parameters other than propeller pitch are constant. Wageningen B-series propellers give researchers a chance to study the effect of propeller pitch in detail; the series allows propeller pitch, blade area ratio and blade number modification. A wide range of open-water tests were performed on the series and made available by Oosterveld and Van Oosanen (1975). A polynomial regression analysis was also conducted and open-water diagrams of about 1,000 propellers presented in the report by Bernitsas et al. (1981). The current paper addresses the gap in the current knowledge on CPP interaction with the hull in terms of ship propulsion by the integration of Wageningen B-series propellers and SPE.

The paper is organized as follows. Section 2 explains SPE, the Wageningen B-Series propeller database, and the main code connecting both. Method validation on model and full-size ships is presented in Section 3. Section 4 gives a brief account of towing tank experiments conducted for KCS and DTC. Total resistances of selected ships have been used as one of the inputs of the method. This section is also devoted to the assessment of open-water test results conducted at different ship model testing laboratories. Section 5 compares the open-water performances of available experimental results and generated propellers. Results and discussion are presented in Sections 6 and 7, respectively. Finally, the main results of the study are briefly summarized in Section 8.

## 2. METHODOLOGY

The developed method consists of the SPE method explained in literature and the newly introduced Wageningen B-series propeller generator. Parameter resistance values used in the developed method were obtained experimentally, open water propeller coefficients from the Wageningen B-series propeller database, and  $t$  and  $w$  from experimental results found in the literature.

### 2.1. Self-propulsion Estimation Method

The SPE method used in this study is novel and has only recently been published in literature (Kinaci et al.; 2018), (Kinaci

et al.; 2020). The method examines hull-propeller interactions and iteratively calculates propeller rotation rate. It is similar to the direct method  $K_T/J^2$  recommended by the ITTC (2017a), where this auxiliary equation is used in a similar fashion to predict self-propulsion parameters (Birk; 2019). The SPE differs from the 1978 ITTC Performance Prediction Method in two respects:

- SPE is a more practical tool since open-water propeller performance is expressed mathematically. 1978 ITTC Performance Prediction Method uses a graph to find the intersection of  $K_T = C_s J^2$ , where  $C_s$  is an additional parameter named "shortened thrust loading coefficient".
- In 1978 ITTC Performance Prediction Method the unknown propeller rotation rate  $n$  is eliminated by dividing the thrust coefficient equation by advance coefficient. The SPE method is programmed to iteratively calculate  $n$ .

The SPE implicitly assumes that the relative-rotative efficiency of the propeller is  $\eta_R = 1$ . This is considered to be a fair assumption as this value is generally in the  $0.98 < \eta_R < 1.02$  range for conventional displacement hull forms.

The iterative nature of the self-propulsion estimation method is extensively explained in Kinaci et al. (2020) and the details will not be included in this study. Instead, the fundamental equations used in SPE will be presented in further text. Thrust should be equal to resistance for a ship to move at a certain velocity. The total resistance  $R_T$  of the ship should be equal to propeller thrust  $T$ , also bearing in mind the interactions taking place between the hull and the propeller. This can mathematically be expressed as

$$R_T = T(1 - t) \quad (1)$$

where  $t$  is the thrust deduction factor. Thrust ( $T$ ) and torque ( $Q$ ) values in self-propulsion tests are expressed in non-dimensional forms as thrust ( $K_T$ ) and torque coefficients ( $K_Q$ ), respectively:

$$K_T = \frac{T}{\rho n^2 D^4} \quad (2)$$

$$K_Q = \frac{Q}{\rho n^2 D^5} \quad (3)$$

where,  $n$  is model propeller revolution speed,  $D$  the diameter of the model propeller and  $\rho$  water density. Open-water propeller efficiency is calculated as follows

$$\eta_o = \frac{J}{2\pi} \frac{K_T}{K_Q} \quad (4)$$

Thrust identity is used to calculate the self-propulsion parameters of the ship by means of the propeller's advance coefficient. Advance coefficient  $J$  is defined as

$$J = \frac{V(1-w)}{nD} \quad (5)$$

where  $w$  is wake fraction. Detailed information on data reduction equations and extrapolation method can be found in ITTC (2017c, 2017a).

## 2.2. The Structure of the Developed Method

The Wageningen B-series propeller database includes propellers with different numbers of blades,  $Z$ , blade area ratios,

$A_E/A_0$ , and pitch ratios,  $P/D$ . The performances of approximately 1,000 propellers were obtained from the extensive tests carried out in Wageningen (Oosterveld and Van Oosanen; 1975). The database is an exceptionally practical way to generate new propellers, including their open-water performances. In the present study, all experimental results were collapsed into mathematical expressions by polynomial regression analysis. Finally, new propellers with different pitch ratios were generated using the database.

The database was integrated into the self-propulsion estimation code by applying second order polynomial coefficients. Thrust, torque and efficiency curves, as well as mathematical expressions obtained from polynomial regression analysis area available in Bernitsas, et al. (1981). The SPE code was improved to change  $k_0$ ,  $k_1$  and  $k_2$  constants of  $K_T$  and  $g_0$ ,  $g_1$  and  $g_2$  constants of  $K_Q$  curves depending on propeller changes. A Wageningen B-series propeller generator code was also developed to generate new propellers, and provide input for the "open-water propeller performance" section of the SPE code. Two stand-alone codes, i.e. self-estimation code and Wageningen B-series propeller generator, work together through the main code to account for self-propulsion parameter changes. The flow diagram of the main code is given in Figure 1.

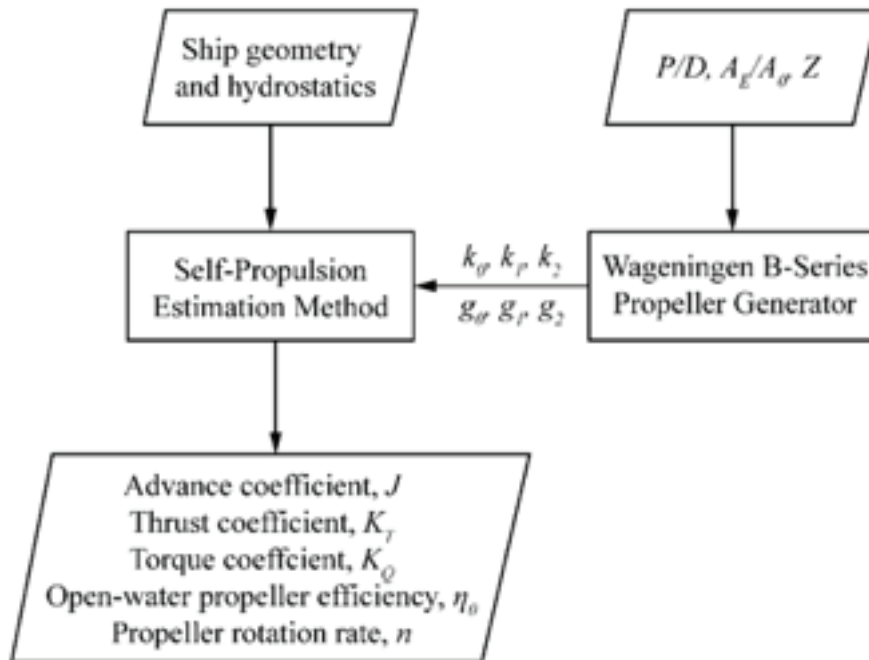


Figure 1. Flow chart of the main code running two stand-alone sub-codes.

Apart from the hydrostatic and geometric properties of the hull, the code requires four additional inputs: bare hull resistance ( $R_T$ ), open-water propeller performance ( $k_0$ ,  $k_1$ ,  $k_2$ ,  $g_0$ ,  $g_1$  and  $g_2$  coefficients), thrust deduction factor ( $t$ ), and wake fraction ( $w$ ). Bare hull resistance can be stated with or without the rudder depending on the choice of computation. Hull-propeller interactions have been embedded in the method using the wake fraction,  $w$ , and thrust deduction factor,  $t$ . Open-water propeller performance is provided as input using the coefficients of second order approximations of thrust and torque coefficient curves ( $K_T = k_0 + k_1 J + k_2 J^2$  and  $K_Q = g_0 + g_1 J + g_2 J^2$ ). Self-propulsion parameters are viewed in the "Results" section after clicking on the "Calculate" field. The code can predict ship propeller rotation rate using a model ship, with skin friction coefficient (SFC) calculated during the procedure. Since full size ships were preferred in this study, SFC calculation was not required.

The computer program with a graphical user interface was coded in MATLAB to facilitate the implementation of the method. The graphical user interface of the code based on the SPE method is presented in Figure 2. Values in the figure pertain to a full size DTC ship with its original propeller.

The code increases propeller rotation rate until the balance between the thrust generated by the propeller and total ship resistance is achieved. In the case given in Figure 2, propeller thrust (315 kN) exceeds total ship resistance (312 kN) by approximately

1%. Changes in the third digit of the propeller rotation rate would lower this difference but this level of precision is considered to be sufficient. The assumptions made in SPE are as follows:

- The relative rotative efficiency of the propeller is 1, i.e.,  $\eta_R \approx 1$ .
- The ship is considered to be moving only in the forward direction, neglecting the effects of heave, pitch, and roll.
- Scale effect corrections in  $K_T$  and  $w$  are not considered (Sezen et al., 2021).

Thrust deduction factor and wake fraction may be defined as a function of other parameters in SPE. In the present study, the parameters were taken as constants since self-propulsion parameters are not that sensitive to  $w$  and  $t$ . The sensitivity analysis where  $w$  was increased or decreased by 10% revealed that propeller rotation rate  $n$  changed by only 1.4%. The same procedure yielded a 0.4% change in  $n$  for a 10% change in  $t$ . Taking the parameters as a constant is therefore believed to be a reasonable assumption.

It should also be noted that while cavitation is not considered in this study, SPE is capable of incorporating the effects of cavitation on ship self-propulsion. A cavitating propeller will generate different coefficients of thrust and torque curves ( $k_0, k_1, k_2, g_0, g_1$ , and  $g_2$ ) in open-water propeller tests, which will eventually change self-propulsion parameters.

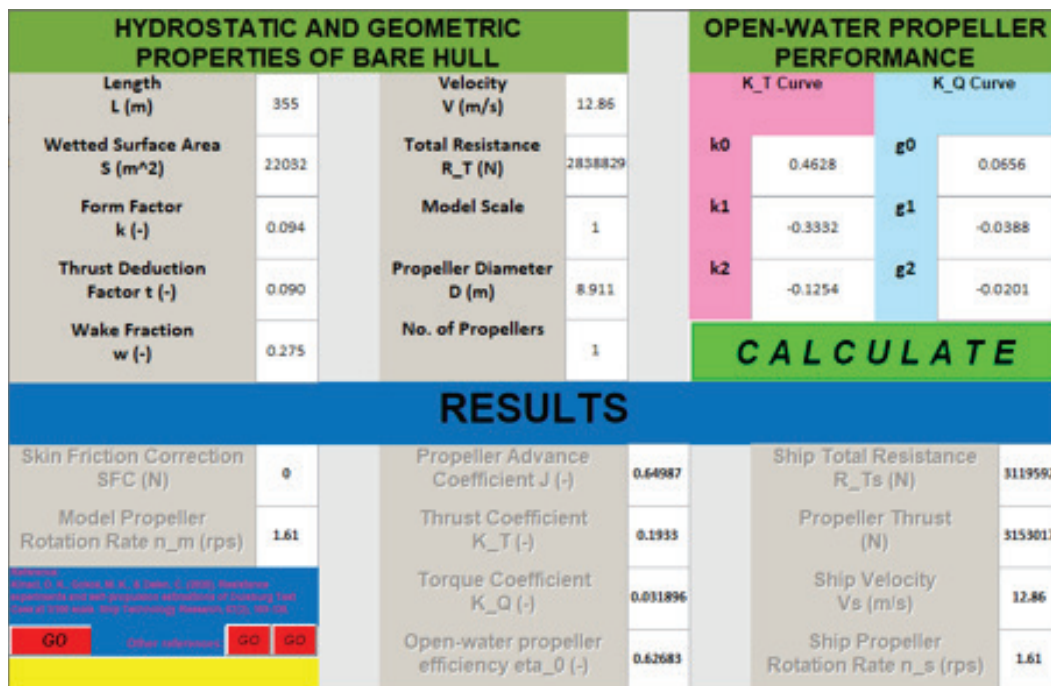


Figure 2. SPE graphical user interface.

### 3. SPE METHOD VALIDATION STUDIES

The self-propulsion estimation method was validated several times using different benchmark ships, such as DARPA Suboff, 1/31.6 KCS scale model and 1/59.407 DTC scale model in Kinaci et al. (2018); Japanese Bulk Carrier (JBC) in Gokce et al. (2019) and 1/80 DTC scale model in Kinaci et al. (2020). A new KCS self-propulsion validation study conducted on a different scale model (1/60.75) was provided to ensure the integrity of the present study. SPE module inputs are presented in Table 1.

The comparison of SPE results with self-propulsion test results taken from Carrica et al. (2010) are given in Table 2. As can

be seen from the table, the correspondence between SPE and experiment results is remarkable.

The main purpose of the study is to examine the impact of the changes in propeller pitch on ship propulsion on a full size ship. Prior to making fundamental estimations, the SPE method was also assessed on a full size Seiun Maru ship, whose sea trial results are available in literature. Seiun Maru is a  $L_{pp}=105$  m long ship with propeller diameter of  $D=3.6$  m. The ship was built in 1997 and is still being used for training purposes by the Japanese government. The hydrostatic and geometric properties of the ship have been obtained from Ukon et al. (1989) and presented in Table 3.

**Table 1.**  
SPE code inputs.

L	3.786 m	V	1.584 m/s				
S	2.585 m <sup>2</sup>	R_T	14.16 N	$k_0$	0.4720	$g_0$	0.0688
k	0.1	$\lambda$	60.75	$k_1$	-0.3073	$g_1$	-0.0358
t	0.147	D	0.13 m	$k_2$	-0.1354	$g_2$	-0.2290
w	0.208	No. Pr.	1				

**Table 2.**  
Comparison of SPE results with KCS self-propulsion experiments at  $Fr=0.26$ .

	J	$K_T$	$K_Q$	$\eta_0$
EFD (Carrica et al., 2010)	0.728	0.170	0.029	0.682
SPE (Present study)	0.734	0.173	0.030	0.672
Percentage error (%)	0.824	1.765	3.448	1.466

Since the thrust deduction factor  $t$  of the ship is not provided, estimated IMO ( $t=0.7w$ ) was used (IMO; 2013) to determine  $t=0.127$ . The propeller of the Seiun Maru can be recreated by using Wageningen B-series propellers, given that they have similar open-water propeller performances, stated in Belhenniche et al. (2016). During sea trial tests, propeller thrust  $T$  was measured and indicated in Table 4 for each ship speed. Total resistance  $R_T$  of the ship can be calculated from the data provided by using the equation  $R_T=T \cdot (1-t)$ . Thus, measured data

have been used as an input to meet the bare hull total resistance requirement in SPE.

Self-propulsion parameters can be estimated using geometric parameters of the ship from Table 3, open-water performance dataset of Wageningen B-series propellers, and propeller thrust given in Table 4. The comparison of propeller rotation rates and thrusts obtained by the self-propulsion estimation method and by sea trials is presented in Figure 3. The tabular values of the graphs in this figure and error percentages are given in Table 5.

**Table 3.**

General properties of the full size Seiun Maru ship and its propeller.

Length between perpendiculars	$L_{PP}$	m	105
Waterline length	$L_{WL}$	m	108.95
Breadth	B	m	16
Draft	T	m	5.8
Displacement	$\nabla$	$m^3$	5781.3
Wetted area	S	$m^2$	2127.9
Block coefficient	$C_B$	-	0.576
Number of propellers	-	-	1
Propeller diameter	D	m	3.6
Number of propeller blades	Z	-	5
Propeller pitch ratio	P/D	-	0.95
Propeller blade area ratio	$A_E/A_0$	-	0.65
Wake fraction	w	-	0.182

**Table 4.**

Propeller thrust measured during sea trial tests on the Seiun Maru.

Ship speed	knots	7.2	9.1	10.5	14.5	15.7
Propeller thrust	kN	53.955	80.442	127.53	230.535	269.775

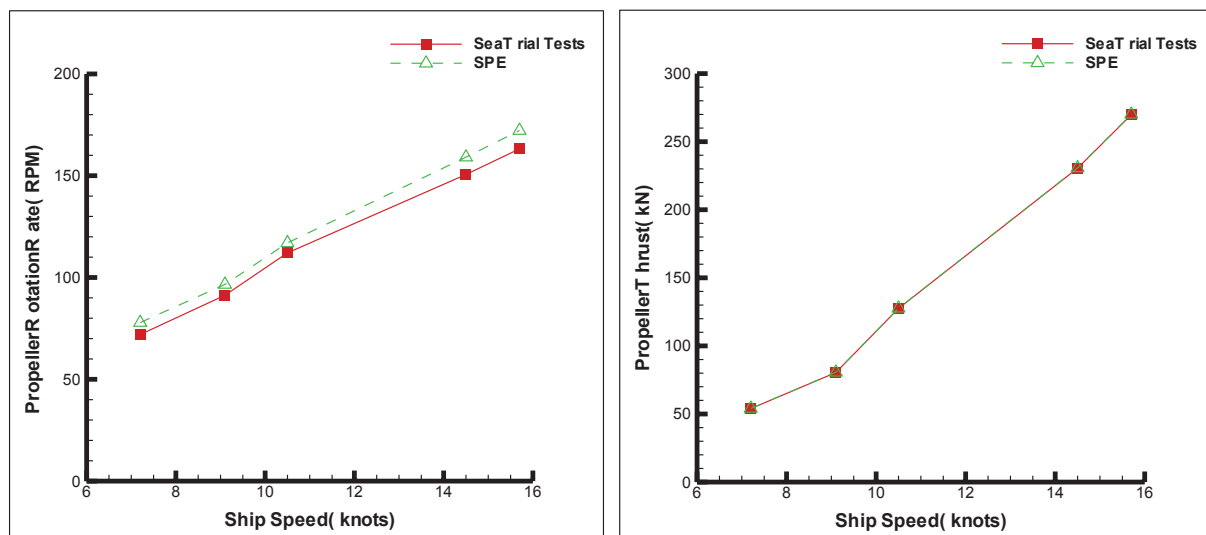


**Figure 3.**

The Seiun Maru sea trial tests vs. SPE in terms of propeller rotation rates (left) and propeller thrust (right) with respect to ship speed.

**Table 5.**

Tabularized values of propeller rotation rates and thrust given in Figure 5.

Ship speed	Thrust			Propeller rotation rate		
	SPE	Sea trial	Difference	SPE	Sea trial	Difference
knots	N	N	%	rpm	rpm	%
7.2	54.058	53.955	-0.190	77.9	72.0	-8.167
9.1	80.602	80.442	-0.199	96.6	91.3	-5.805
10.5	127.684	127.530	-0.121	117.0	112.1	-4.371
14.5	230.735	230.535	-0.087	159.1	150.6	-5.657
15.7	270.090	269.775	-0.117	172.2	163.2	-5.515

#### 4. EXPERIMENTAL STUDY

The total resistance of the ship and open-water propeller curves are required inputs in the SPE method used in this study. Test results will be used to calculate the self-propulsion parameters by the application of SPE. While resistance tests were conducted for KCS and DTC container ships, open-water propeller tests were performed for the DTC's propeller. Ship resistance and open-water propeller performance experiments were carried out at the Ata Nutku Ship Model Testing Laboratory at the Istanbul Technical University.

##### 4.1. Resistance Tests

Resistance tests, as stated in ITTC (2017a), were based on the measurement of the resistance force generated by the model against the fluid as the hull advances at a constant Fr number. The total resistance coefficient of the scale model ship ( $C_{TM}$ ) was expressed by the towing force ( $R_{TM}$ ) measured in the tests as follows:

$$C_{TM} = \frac{R_{TM}}{0.5\rho_M S_M V_M^2} \quad (6)$$

where  $\rho_M$  is fluid density,  $S_M$  is the wetted surface of hull and  $V_M$  is the advance velocity of the hull. The sub-index M denotes the scale model. Model tests were carried out to determine the correlation between the Fr number and the wave-making resistance coefficient ( $C_{WM}$ ) of the model. Regardless of the

differences in scales,  $C_{WM}$  is considered equal to  $C_{WS}$  and is used in the estimation of total resistance at full scale. Hughes approach to model wave resistance calculation can be expressed as

$$C_{WM} = C_{WS} = C_{WM} - (1+k)C_{FM} = C_W \quad (7)$$

where (1+k) is the form factor calculated by the Prohaska method.  $C_{FM}$  is derived from the ITTC-1957 model correlation line using the corresponding Re number of the model as follows:

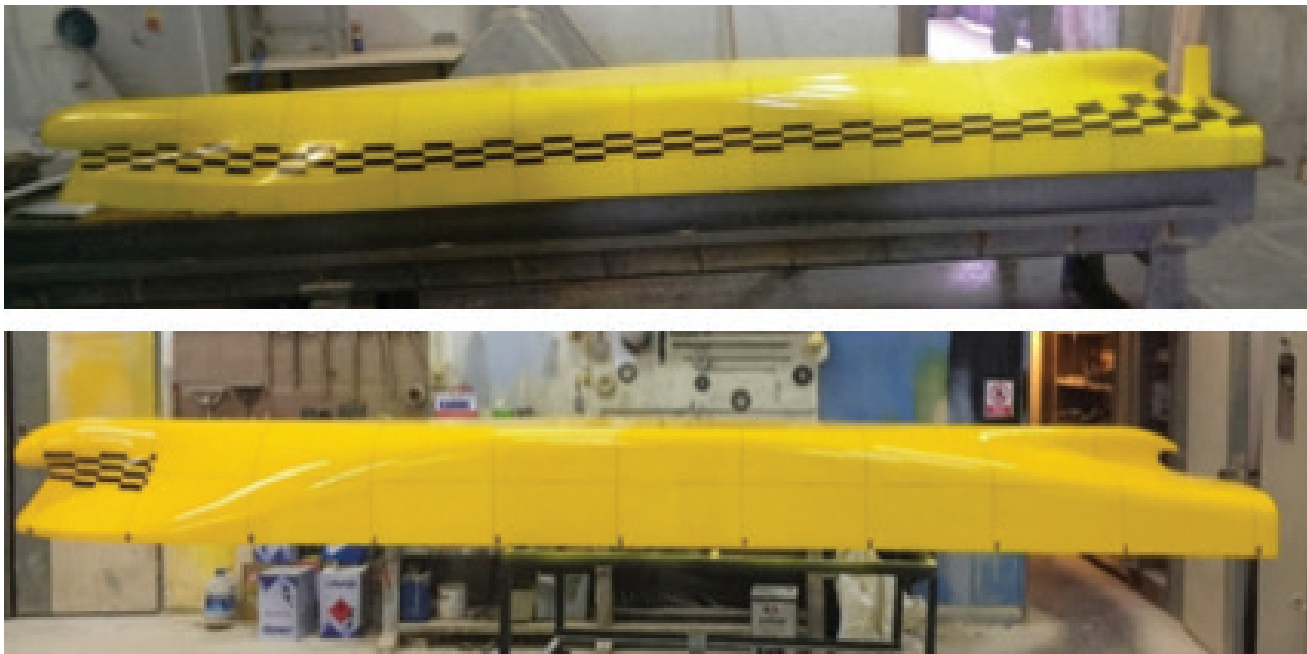
$$C_{FM} = \frac{0.075}{(\log Re_M - 2)^2} \quad (8)$$

Two modern ship hulls, KCS and DTC, frequently used to validate and verify CFD applications, were selected to predict full size propulsive characteristics using the SPE method. The KCS hull is a modern container ship with bulbous bow designed by the Korea Research Institute of Ships and Ocean Engineering (Van et al. 1998; Kim et al., 2001). The DTC is the hull design of the 14,000 TEU container ship developed by the Institute of Ship Technology, Ocean Engineering and Transportation Systems (el Moctar et al., 2012). A 60.75 scale KCS hull and an 80 scale DTC hull were manufactured in the workshop of the ITU Ata Nutku Ship Model Testing Laboratory in accordance with recommended procedures and guidelines of the ITTC (2017c). Their main dimensions and characteristics are given in Table 6. Profile views of the manufactured KCS and DTC models are shown in Figure 4.

**Table 6.**

Principal particulars of KCS and DTC hulls.

	Z	P/D	$A_E/A_0$	$k_0$	$k_1$	$k_2$	$g_0$	$g_1$	$g_2$
HSVA	5	0.997	0.8	0.4951	-0.4338	-0.0918	0.0717	-0.0520	-0.0165
KRISO	5	0.964	0.818	0.5505	-0.4466	-0.0930	0.0762	-0.0523	-0.0158
MARIN	5	0.997	0.748	0.4720	-0.3073	-0.1354	0.0688	-0.0358	-0.0229
SVA Potsdam	5	0.959	0.8	0.4628	-0.3332	-0.1254	0.0656	-0.0388	-0.0201
Ata Nutku	5	0.959	0.8	0.4892	-0.3580	-0.0690	0.0738	-0.0456	-0.0116
Generated	5	0.997	0.8	0.4822	-0.3303	-0.1265	0.0708	-0.0400	-0.0209

**Figure 4.**

Profile views of the KCS (top) and the DTC (bottom) hulls.

Experimental resistance tests conducted on the bare DTC and KCS models with rudders were carried out at the Ata Nutku Ship Model Testing Laboratory (SMTL) of the Istanbul Technical University, in accordance with ITTC recommended procedures and guidelines (2017d). The towing tank is 160 m long, 6 m wide and has the water depth of 3.5 m. The maximum velocity of the towing carriage is 5.5 m/s. Since the width of the towing tank

exceeds  $0.36 \times L_{WL}$ , the sidewall effects on results are negligible (Yuan et al., 2018). The models were adjusted to be free to heave and pitch motions in the towing carriage. The horizontal force acting on the model was measured from the LCF point of the models. When the models were advancing at constant design velocity, model resistance signals were stored simultaneously. The measured resistance values were modified, based on ITTC

recommendations (2014a), to 15°C water temperature. They were extrapolated to the ship scale using the ITTC (2017d, 2017a) methods as given in Table 7. Values of the ship scale were calculated by extrapolation of the scale model test results. In the table, the sub-index S represents a full size ship.

In the second part of the study, the effect of ship speed was examined on KCS. Experimental results at different speeds extrapolated to full size KCS are presented in Table 8.

**Table 7.**

KCS and DTC resistance coefficients at service speeds.

Hull	Model					Ship				
	$V_M$ (m/s)	$C_{FM} \times 10^3$	$C_{VM} \times 10^3$	$C_W \times 10^3$	TM $\times 10^3$	$V_{m/s}$	$C_{FS} \times 10^3$	$C_{VS} \times 10^3$	$C_W \times 10^3$	TS $\times 10^3$
KCS	1.584	3.365	3.701	0.669	4.371	12.35	1.371	1.508	0.669	2.177
DTC	1.438	3.326	3.644	0.137	3.781	12.86	1.297	1.421	0.137	1.558

**Table 8.**

Experimental results of KCS bare hull resistance coefficients extrapolated to full-scale.

V	V	Fr	$C_T \times 10^3$
knots	m/s	-	-
19.40	9.98	0.21	1.684
24.00	12.35	0.26	2.177
25.84	13.29	0.28	2.817
28.61	14.72	0.31	4.201

The experimental uncertainties of model ships used at the Ata Nutku SMTL were previously calculated and published in literature. Delen and Bal (2015) estimated the experimental uncertainties of the KCS hull using ITTC guideline (2014b, 2014c). The expanded resistance test uncertainty in the design of the Fr number of the KCS hull was predicted as 1.16% with 95% confidence. Additionally, the experimental uncertainty of the 1/100-scale DTC model was found to be 1.10% with 95% confidence in Kinaci et al. (2020).

#### 4.2. Open-water Propeller Tests

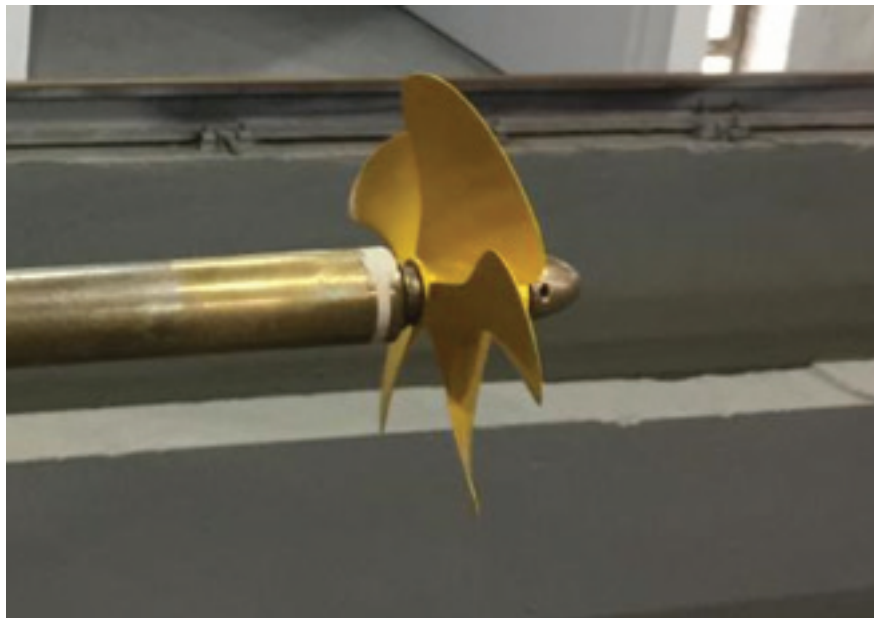
Open-water propeller tests for the DTC propeller were conducted on a 1/80 scale model having the propeller diameter of  $D=11.1$  cm. The propeller model given in Figure 5 was constructed using a 3D printer with the printing volume of  $200 \times 200 \times 200$  mm. After the printing process, the propeller was covered with paste, ground to remove surface roughness, and painted to make it ready for open-water tests. The propeller was mounted on a slender ship model and submerged to the desired depth of  $1.5D$  as recommended by the ITTC (2017b).

The propeller was located at a distance from the ship with the help of a long shaft so as not to be affected by pressure and velocity distribution around the model. All motions of the model were restricted during the experiments. During the experiment, the inflow velocity on the propeller, propeller revolution rate, thrust, and momentum values generated by the propeller were collected instantaneously. Propeller advance coefficient was varied by fixing the propeller rotation rate and modifying inflow velocity.

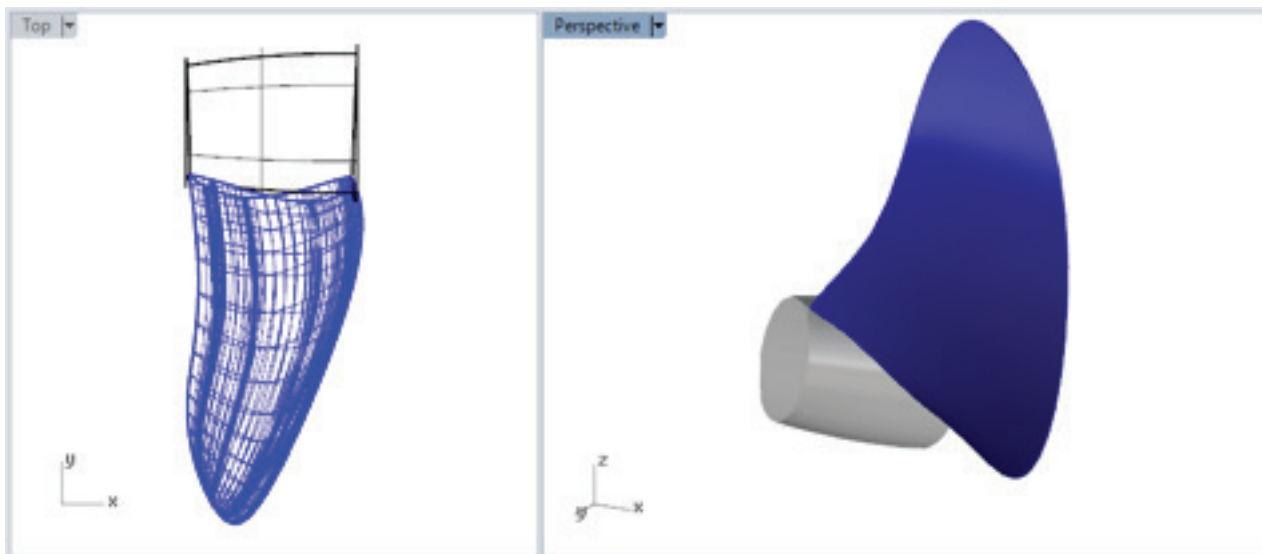
The uncertainty analysis in the experimental study was carried out by examining only the precision limit of thrust and torque values. The precision limits ( $P_{(T \& Q)} = Ks/\sqrt{M}$ ) of open water experiments have been determined for repeated tests.  $M=3$  is the number of runs for which the precision limit is to be established,  $s$  is the standard deviation of thrust and torque results established by multiple runs, and  $K=2$  is the coverage factor. The precision limits of thrust and torque results are estimated as 0.641% and 0.841%, respectively. Experiment results and geometric details of the propeller are given in the following text.

KCS and DTC propellers are almost identical in that they are 5-blade fixed pitch propellers with the blade area ratio of 0.8 and the pitch ratio of approximately 1. The geometric comparison of these two propellers is illustrated in Figure 6. Four upper and lower left images show one blade of the KCS propeller (in blue), while the other four upper and lower right images show the DTC propeller (in red). The lowest image shows the superposition of the two blades. The SIMMAN website provides three different experimental results for the KCS propeller conducted at HSVA,

KRISO, and MARIN (<http://www.simman2019.kr/contents/KCS.php>). El Moctar et al. (2012) published open-water test results for the DTC propeller. The geometric properties of the propeller tested at each towing tank are presented in Table 9. As can be seen in the table, there are slight differences between geometric properties of the propellers. KRISO provides two open-water results, both for the scale model and the full size propeller. KRISO's full size propeller results were considered in the present study.



**Figure 5.**  
A view of the 1/80 scale model DTC propeller.



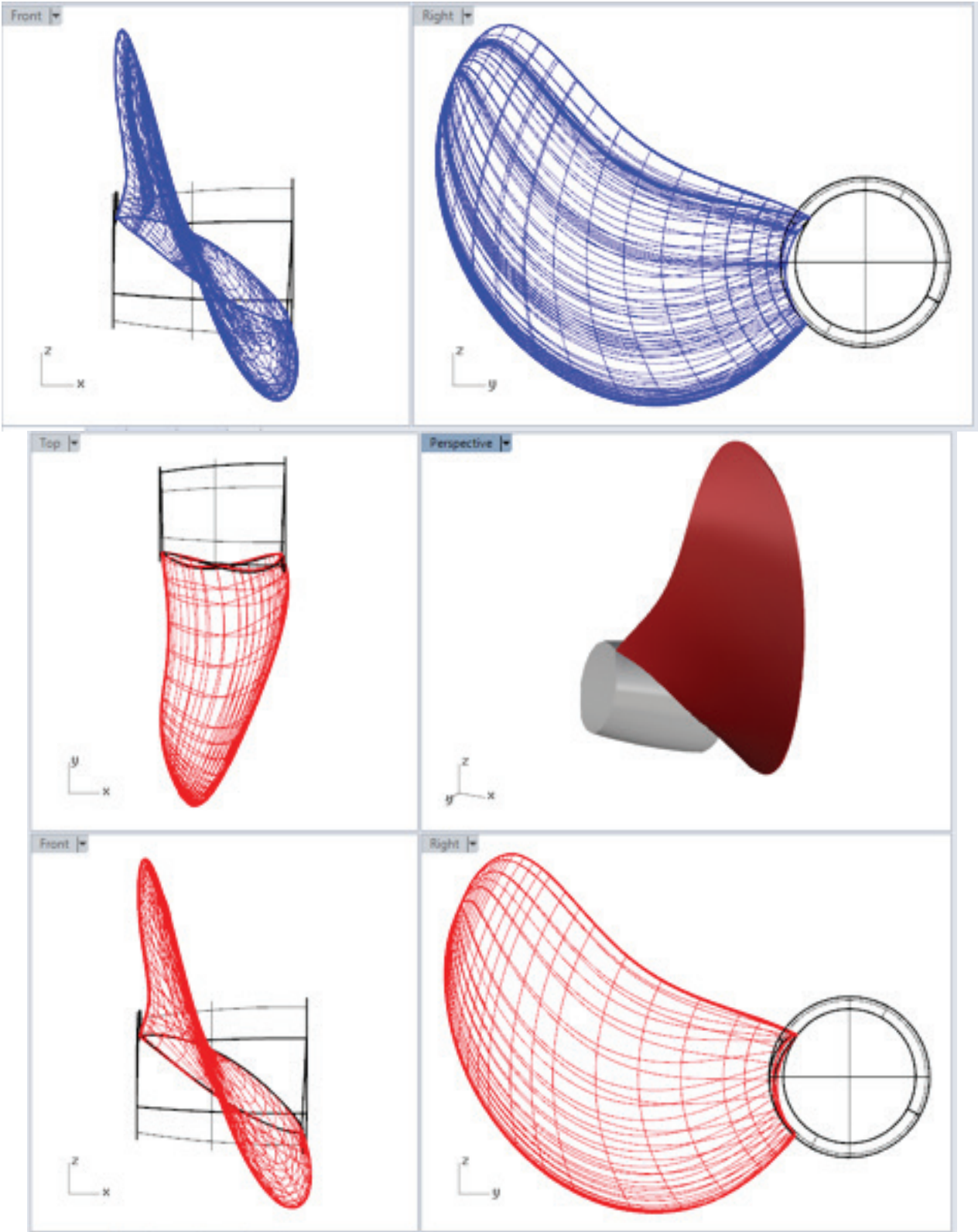




**Figure 6.**  
Geometric comparison of blades: the KCS propeller in blue and the DTC propeller in red.

**Table 9.**  
Geometric properties of propellers tested in open-water in different towing tanks.

	Original full size propellers		Experimental conditions in				
			HSVA	KRISO	MARIN	Ata Nutku	SVA Potsdam
Propeller	KCS	DTC	KCS	KCS	KCS	DTC	DTC
Type	Fixed pitch	Fixed pitch	Fixed pitch	Fixed pitch	Fixed pitch	Fixed pitch	Fixed pitch
No. of blades	5	5	5	5	5	5	5
D (m)	7.9	8.911	0.105	7.9	0.2085	0.111	0.15
P/D (0.7R)	0.997	0.959	0.997	0.964	0.997	0.959	0.959
$A_E/A_0$	0.8	0.8	0.8	0.818	0.748	0.8	0.8
Rotation	Right hand	Right hand	Right hand	Right hand	Right hand	Right hand	Right hand
Hub ratio	0.18	0.176	0.18	0.18	0.186	0.176	0.176

## 5. HYDRODYNAMIC PERFORMANCE OF GENERATED PROPELLERS

A propeller was generated by conducting the polynomial regression analysis on the tests carried out at the Netherlands Ship Model Basin in Wageningen (Oosterveld and Van Oosanen; 1975). Generation parameters were selected to be similar to the original propeller geometry, namely  $Z=5$ ,  $P/D=0.997$ , and

$A_E/A_0=0.8$ . The comparison of open-water propeller experiment results with the open-water performance of the generated propeller (using Wageningen B-Series propeller database) is given in Figure 7. The experimental results of KRISO, MARIN, SVA Potsdam, and Ata Nutku are similar, while HSVA shows some discrepancies. Likewise, the open-water performance of the generated propeller seems to correspond to KRISO, MARIN, SVA Potsdam, and Ata Nutku experimental results.

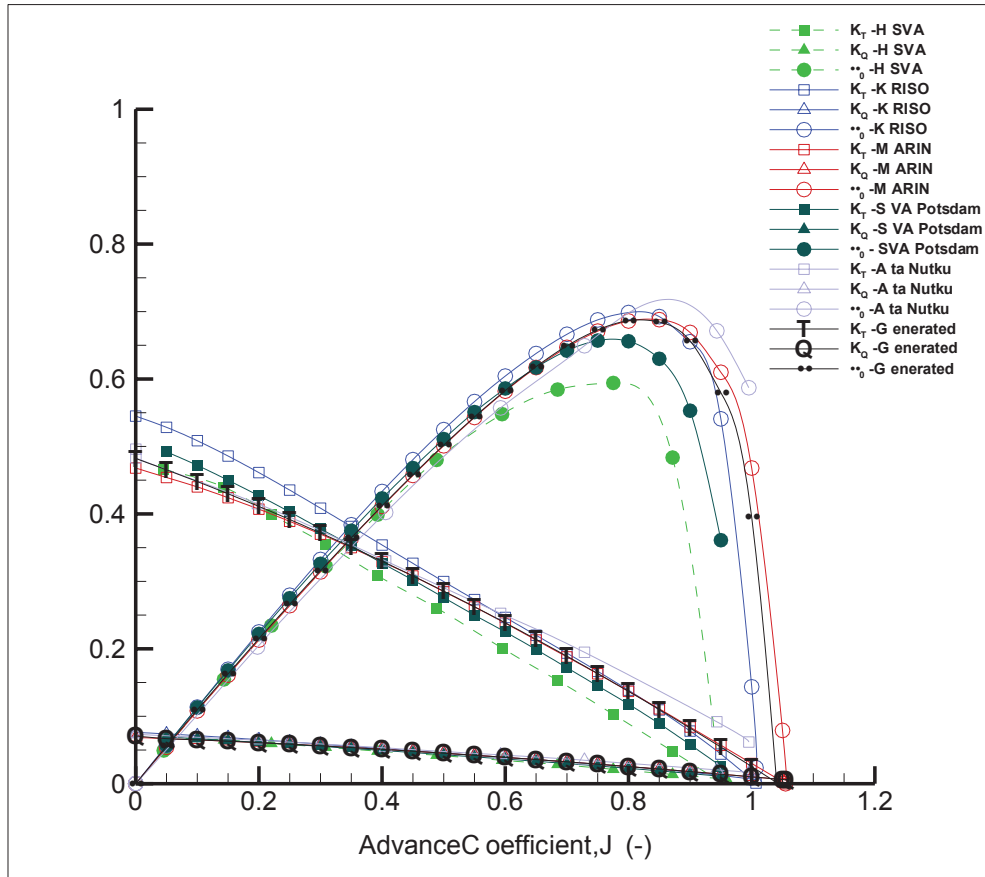


Figure 7.

Open-water experiments on the KCS propeller conducted at different towing tanks compared to the generated propeller.

Thrust and torque coefficients of open-water results are expressed as a second-order polynomial function of the advance coefficient,  $J$ . Coefficients have been obtained using

$$K_T = k_0 + k_1 J + k_2 J^2 \quad (9)$$

$$K_Q = g_0 + g_1 J + g_2 J^2 \quad (10)$$

after the curve fitting process. Curve fitting results used to obtain open-water coefficients are summarized in Table 10. The comparison of coefficients given in the table reveals that the generated propeller resembles the experiments carried out at MARIN.

After comparatively examining the open water performance of the propeller manufactured to have the same specifications as the KCS (or DTC) propeller, the pitch ratio values of the newly manufactured propellers have been changed. Using the experimental database provided by Oosterveld and Van Oosanen (1975), 10 Wageningen B-series propellers were manufactured whose pitch was changed between  $0.5 < P/D < 1.4$ . In other words, the  $P/D$  was changed during production, while other parameters were kept constant ( $Z=5$  and  $A_E/A_0=0.8$ ). Open-water coefficients of generated propellers are given in Table 11.

Using the values provided in Table 11, open-water diagrams of all propellers can be obtained. The open-water performances of four propellers, having the pitch ratios of 0.5, 0.8, 1.1 and 1.4 are presented in Figure 8. It can be stated from the figure that maximum open-water propeller efficiency  $\eta_0$ , increases with the pitch ratio,  $P/D$ .

**Table 10.**

Coefficients obtained from curve fitting open-water propeller performance.

	Z	P/D	$A_E/A_0$	$k_0$	$k_1$	$k_2$	$g_0$	$g_1$	$g_2$
HSVA	5	0.997	0.8	0.4951	-0.4338	-0.0918	0.0717	-0.0520	-0.0165
KRISO	5	0.964	0.818	0.5505	-0.4466	-0.0930	0.0762	-0.0523	-0.0158
MARIN	5	0.997	0.748	0.4720	-0.3073	-0.1354	0.0688	-0.0358	-0.0229
SVA Potsdam	5	0.959	0.8	0.4628	-0.3332	-0.1254	0.0656	-0.0388	-0.0201
Ata Nutku	5	0.959	0.8	0.4892	-0.3580	-0.0690	0.0738	-0.0456	-0.0116
Generated	5	0.997	0.8	0.4822	-0.3303	-0.1265	0.0708	-0.0400	-0.0209

**Table 11.**

Open-water coefficients of all propellers built.

P/D	0.5	0.6	0.7	0.8	0.9	1	1.1	1.2	1.3	1.4
$k_0$	0.2064	0.2616	0.3181	0.3746	0.4302	0.4837	0.5345	0.5819	0.6259	0.6665
$k_1$	-0.2870	-0.2991	-0.3099	-0.3190	-0.3258	-0.3300	-0.3313	-0.3294	-0.3244	-0.3167
$k_2$	-0.1844	-0.1717	-0.1595	-0.1478	-0.1368	-0.1266	-0.1173	-0.1092	-0.1021	-0.0961
$g_0$	0.0187	0.0261	0.0351	0.0457	0.0578	0.0712	0.0858	0.1014	0.1180	0.1354
$g_1$	-0.0184	-0.0229	-0.0273	-0.0316	-0.0359	-0.0401	-0.0443	-0.0483	-0.0520	-0.0550
$g_2$	-0.0125	-0.0147	-0.0168	-0.0185	-0.0199	-0.0209	-0.0215	-0.0217	-0.0218	-0.0221

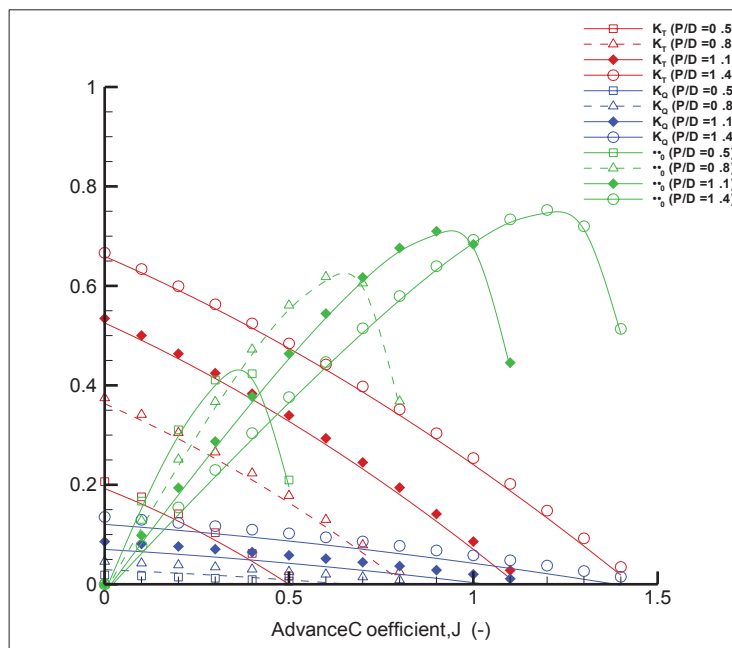


**Figure 8.**

Open-water performances of Wageningen B-Series propellers built.

## 6. RESULTS

The self-propulsion parameters of KCS and DTC ships equipped with a Wageningen B-series propeller, obtained using the self-propulsion estimation method, are presented below. The propeller has five blades ( $Z=5$ ), blade ratio is  $A_E/A_0=0.8$ , and pitch ratio is variable. Both ships have a single propeller. The KCS propeller has the diameter of  $D=7.9$  m, and the DTC propeller the diameter of  $D=8.911$  m. As previously explained in Section 2, the SPE code requires four inputs obtained using the following methods:

- Bare hull resistance,  $R_T$  – experiments conducted at the Ata Nutku SMTL.
- Open-water propeller performance ( $k_0, k_1, k_2, g_0, g_1$  and  $g_2$  coefficients) – the Wageningen B-series propeller database.
- Thrust deduction factor,  $t$  – experimental results published in literature.
- Wake fraction,  $w$  – experimental results published in literature.

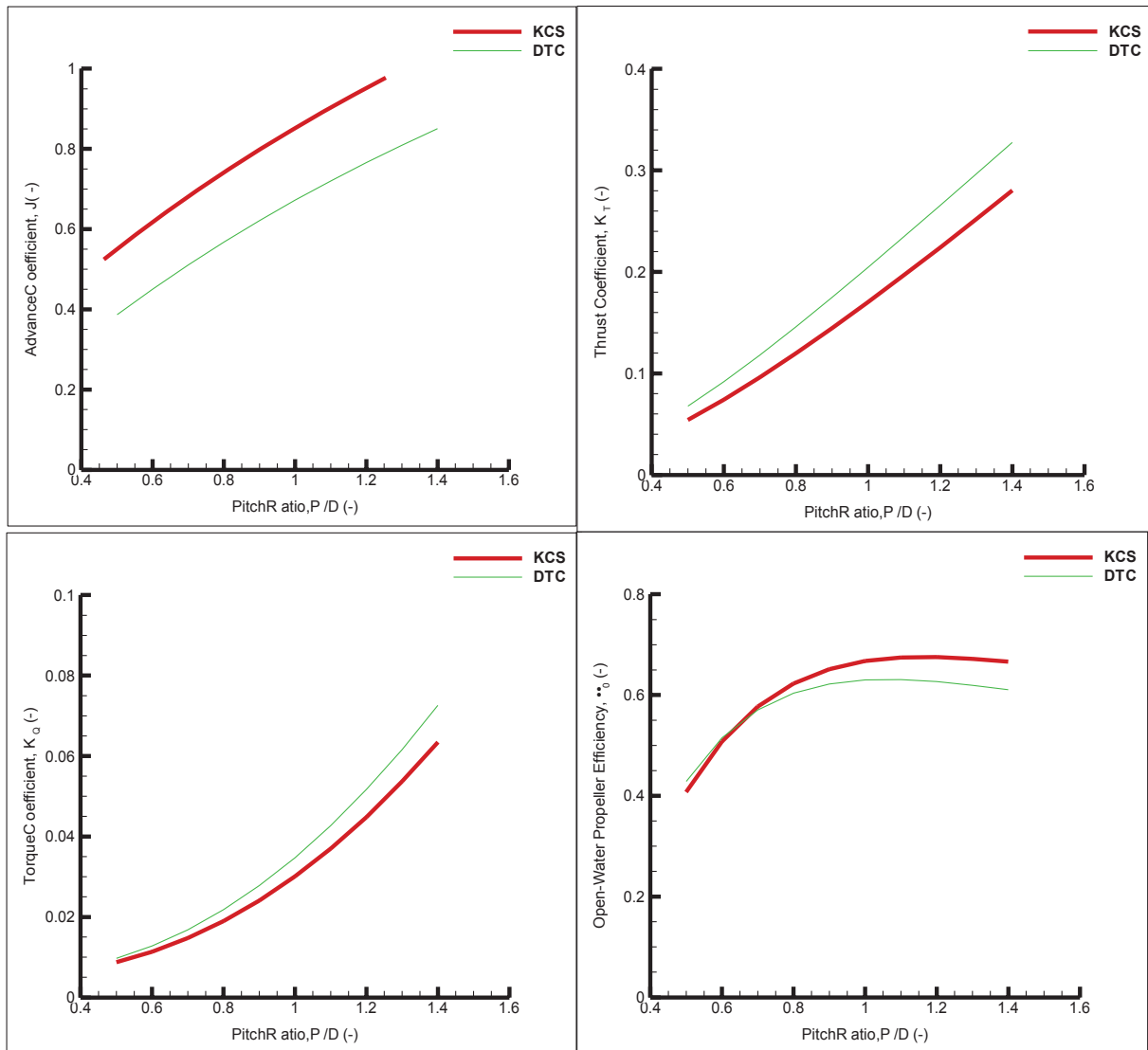


**Figure 9.**

KCS and DTC propulsion parameters at self-propulsion points in correlation with pitch ratio modification P/D. KCS at  $Fr=0.26$ , and DTC at  $Fr=0.218$ .

## 6.1. Propulsion Estimates at Service Speed

First, the self-propulsion parameters for both ships are estimated at their service speeds. Figure 9 shows the self-propulsion predictions obtained for KCS at  $Fr=0.26$  and DTC at  $Fr=0.218$ . The self-propulsion advance coefficient,  $J$ , increases almost linearly in both cases. Changes in  $J$  directly affect other parameters, such as thrust and torque coefficients and increase with increasing pitch ratio. However, it should be noted that the increase in torque coefficient is more drastic, resulting in the reduction of open-water propeller efficiency after a certain  $P/D$ . This matter is directly addressed with the open-water

propeller hydrodynamics. As can be seen in Figure 9, the advance coefficient increases with increasing pitch. When open-water propeller efficiency is past its prime (or optimum point), it starts to decline. Open-water propeller efficiency,  $\eta_0$ , reaches maximum at  $J=1.2$  in KCS, and at  $J=1$  in DTC. After this advance coefficient, the propellers become less efficient. This finding is thought to be particularly important because there is a widespread belief in the field that open-water efficiency increases with increasing propeller pitch. Providing that other total efficiency components remain constant, it can be stated that there is an optimum propeller pitch ratio for ship self-propulsion.

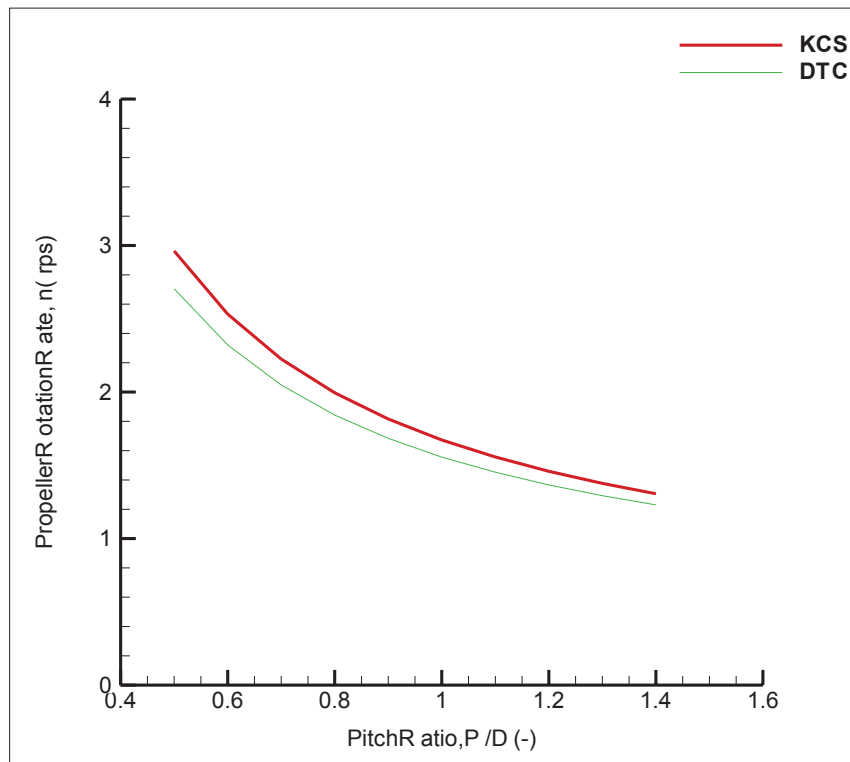


Figure 10.

Propeller rotation rates of KCS at  $V=24$  knots, and DTC at  $V=25$  knots.

The comparison of results of different ships suggests that the propeller is more efficient on KCS. Although the propellers are similar in both ships, hull form plays a fundamental role in the results. Different self-propulsion results obtained for two different ships can be attributed to complex hull-propeller interactions taking place inside the flow. The hull changes the flow around the propeller, causing the propeller to work differently behind the hull. Hull-propeller interactions are generally defined by two parameters, wake fraction,  $w$ , and thrust deduction factor,  $t$ . The

wake fraction,  $w$ , can be defined as a simplified substitute that describes the effect of the hull's form on the propeller. The thrust deduction  $t$ , on the other hand, can be described as the reverse of the wake fraction: it describes the effect of the propeller on the hull. These two parameters for both scale model ships, taken from the experimental results published in literature, are summarized in Table 12. No scale corrections of these parameters were made for full size ships, but were used directly to simplify calculations.

**Table 12.**

Wake fraction and thrust deduction factors for KCS and DTC.

	w	t
KCS (Carrica et al.; 2010)	0.208	0.147
DTC (el Moctar et al.; 2012)	0.275	0.090

As can be seen in Table 12, the wake fraction is lower and the thrust deduction factor greater in KCS. A higher thrust deduction factor might increase ship resistance; however, given that the propeller is the dominant ship propulsion component, any changes in propeller flow would be more significant. Due to lower  $w$ , the propeller receives “better” flow behind KCS, which explains higher open-water efficiency. Propeller rotation rates for both ships at their service speed are given in Figure 10.

SPE validation results were presented in Section 3. The further validation of the method by the comparison of self-propulsion parameters of full size KCS can be presented here. The results of the method used in this study are given in Table 13, along with computational predictions for full size ship

published in literature. As can be seen in the table, the results are somewhat scattered. Advance coefficient range is  $0.71 < J < 0.74$ , thrust coefficient range  $0.165 < K_T < 0.175$  and propeller rotation rate range  $1.67 \text{ rps} < n < 1.74 \text{ rps}$ . The highest discrepancy in results given in Table 13 is the torque coefficient,  $K_Q$ , of the propeller. This is understandable if the relative rotative efficiency is assumed to be one in SPE ( $\eta_r \approx 1$ ). The difference in torque coefficients also has an effect on open-water propeller efficiency,  $\eta_0$ . The discrepancy of some of the results may be attributed to interaction parameters,  $w$  and  $t$ , as they significantly affect self-propulsion parameters. Although experimental values obtained in the scale model experiments were used in the scope of this study, Table 13 gives computations for the full size ship.

**Table 13.**SPE results for full size KCS with its original propeller at  $Fr=0.26$  compared to full size numerical results from literature.

	Method	Rudder	J	$K_T$	$K_Q$	$\eta_0$	n
Present study	SPE	Yes	0.740	0.170	0.0301	0.6672	1.673
Can et al. (2020)	CFD	Yes	0.712	0.175	0.0254	0.7807	1.719
Song et al. (2020)	CFD	Yes	0.714	0.172	0.0276	0.7082	1.703
Song et al. (2020)	CFD	No	0.741	0.158	0.0263	0.7085	1.737
Castro et al. (2011)	CFD	No	0.714	0.166	0.0261	0.7227	1.736

## 6.2. Self-propulsion Parameters Dependent on Changing Ship Speed

KCS self-propulsion parameters dependent on the  $Fr$  number have also been studied. Bare hull resistance values at each ship speed are given in Table 7. The thrust deduction factor and wake fraction values are given in Table 12. Computed KCS self-propulsion parameters dependent on ship speed are illustrated in Figure 11.

Regardless of the pitch ratio,  $P/D$ , of the propeller, the advance coefficient,  $J$ , decreases while the thrust coefficient,  $K_T$ , and the torque coefficient,  $K_Q$ , increase with ship speed. On the other hand, open-water propeller efficiency,  $\eta_0$ , has a dual role. It decreases with increasing speed at high  $P/D$  but acts the

opposite at very low pitch ratios. For fixed pitch propellers, it may have priority in the design phase, as the total efficiency is mostly dependent on open-water propeller efficiency. Another interesting point in the open-water propeller efficiency diagram is that maximum efficiency is different for each  $Fr$  number:

- Maximum  $\eta_0$  for  $Fr=0.21$  case is at  $P/D=1.3$ .
- Maximum  $\eta_0$  for  $Fr=0.26$  case is at  $P/D=1.2$ .
- Maximum  $\eta_0$  for  $Fr=0.28$  case is at  $P/D=1.1$ .
- Maximum  $\eta_0$  for  $Fr=0.31$  case is at  $P/D=1$ .

This suggests that maximum propulsion efficiency changes with ship speed. It is considered important especially for controllable pitch propellers in which ship speed is controlled by propeller pitch modification. Propeller rotation rates are given in Figure 12, while, as anticipated,  $n$  increases with ship speed.

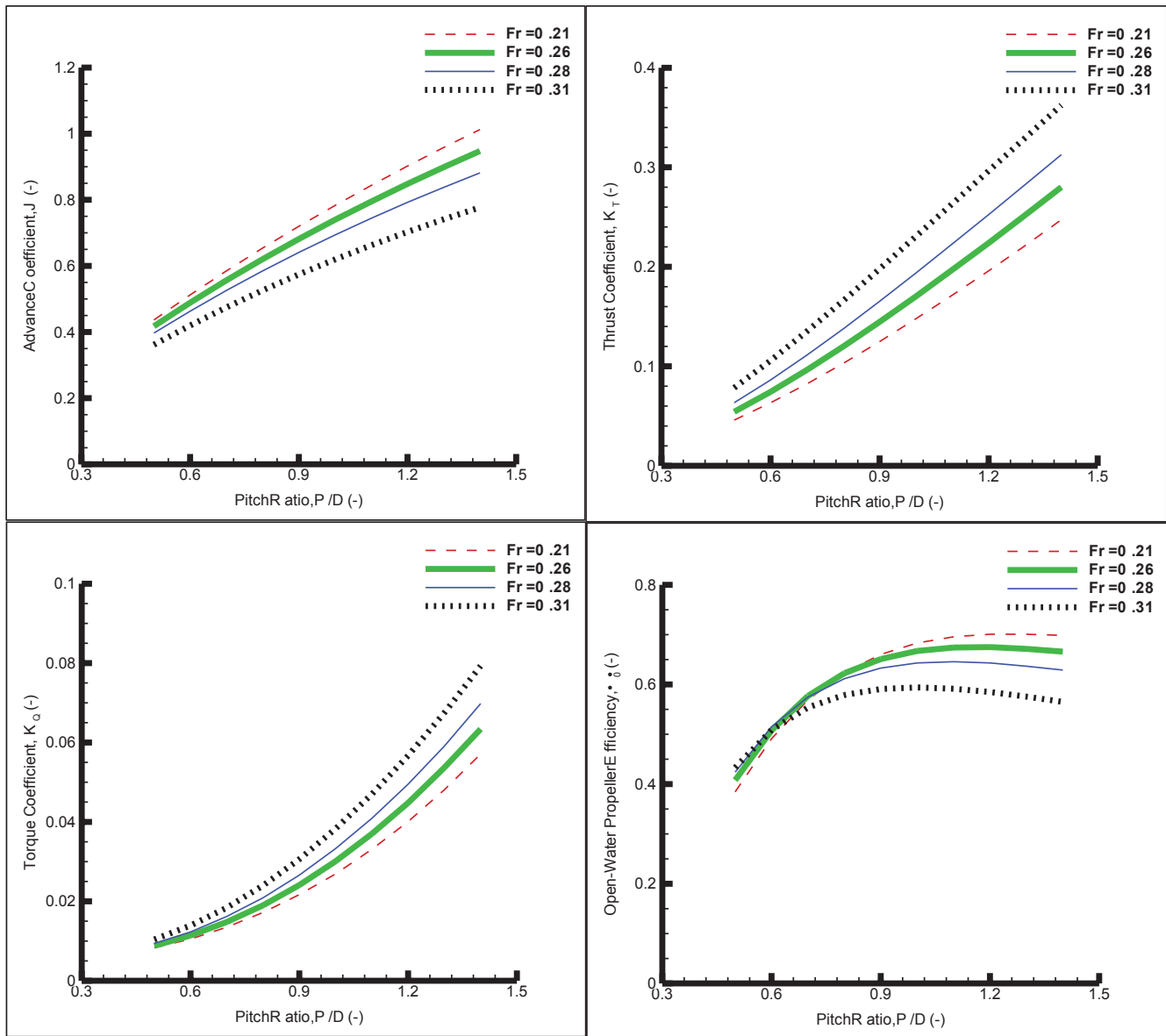
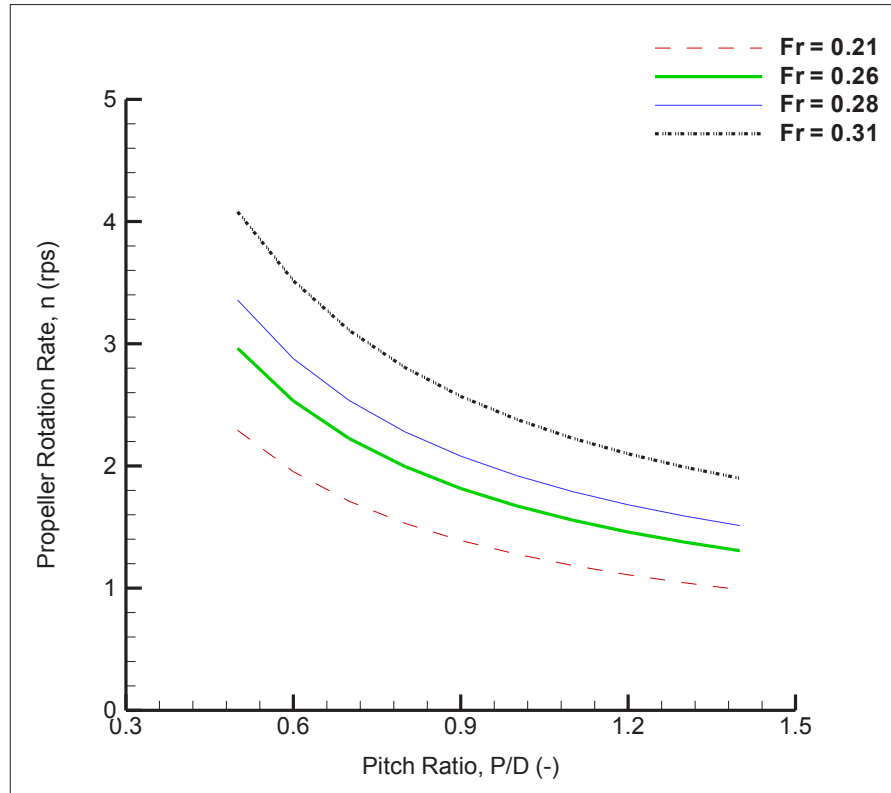


Figure 11.

KCS self-propulsion parameters dependent on changing pitch ratios at different speeds.



**Figure 12.**  
KCS propeller rotation rates at different ship speeds.

## 7. DISCUSSION

Propulsion system selection requires the testing of different propellers, which is both experimentally costly and computationally time-consuming. The self-propulsion estimation (SPE) method that resolves the said issues associated with experiments or CFD-based methods was presented in previous studies. SPE has proven to be a very practical ship propulsion performance assessment method. The method is based on four components that are relatively easy to obtain compared to ship self-propulsion tests on different propellers.

- **Total ship resistance:** The resistance of a ship can be estimated with high accuracy with the application of empirical equations for conventional ships. Additionally, CFD applications and towing tank experiments are straightforward and easier to conduct.
- **Open-water propeller performance:** Once the open-water performance of a propeller is known, the propeller performance can be estimated readily when the propeller is operating behind the hull. Open-water propeller tests are also straightforward and

easier to conduct with either CFD or towing tank experiments. In addition, the performances of Wageningen B-series propellers are already known. An outstanding tool is presented to understand the effect of the geometric properties of the propeller on self-propulsion.

- **Wake fraction:** Wake fraction describes the effect of the ship's hull on propeller performance. This parameter can be estimated with empirical equations or resistance tests. Using sensitivity analysis, the present study established that wake fraction had a relatively lower effect on ship self-propulsion.
- **Thrust deduction factor:** This parameter describes the effect of the propeller on total ship resistance during self-propulsion and can also be estimated with empirical equations. Sensitivity analysis found that the thrust deduction factor had less impact on ship self-propulsion.

The hydrodynamic performance of Wageningen B-series propellers has been known for almost 40 years, during which time they have served as a great tool for understanding ship propulsion. In the study, the series is used to understand the effect of propeller pitch on ship self-propulsion through the

implementation of the SPE method. Thus, the relationship between propeller pitch and ship self-propulsion is revealed. The study has shown that there is an optimum propeller pitch for maximum propulsion efficiency. Additionally, the effect of the Froude number on self-propulsion parameters has also been examined and helped prove that the maximum propulsion efficiency changes with ship speed.

## 8. CONCLUSIONS

Speed variations in ships with controllable pitch propellers are realized by tuning propeller pitch instead of by changing the revolution rate of the main engine. To understand and control CPPs, we need to know the potential consequences of propeller pitch variations on ship self-propulsion. The speed estimation method, recently published in literature, has been enhanced by adding a propeller generator to study the effect of propeller pitch on full size ship propulsion. The method has been validated by sea trial tests conducted on the full size Seiun Maru ship and the correspondence of the results was remarkable. After validating the method, two full size container ships, KCS and DTC, were used, which had similar propellers with the same number of blades, blade area ratios, and nearly the same pitch ratios. The study found that almost identical ship propellers could be generated using the Wageningen B-series propeller database. The results have shown the performance of the generated propeller to be quite similar to that of KCS and DTC propellers, making it a suitable replacement for the original propellers. Once this similarity was established, 10 propellers having different pitch ratios were generated using the B-series database, and the effect of propeller pitch on self-propulsion parameters was investigated.

First, self-propulsion parameters were estimated for both ships with varying P/D ratios at constant service speed. The self-propulsion advance coefficient was found to be increasing almost linearly with the pitch ratio. The thrust and torque coefficients also increased but the increase in torque was greater. The increase in the pitch ratio was found not to continuously increase propeller efficiency. The efficiency reached its maximum at different J values ranging from 1 to 1.2, then decreased after reaching maximum value. Ultimately, ship form had an effect on propeller performance and the propeller operated more efficiently on the KCS than on the DTC. Second, the effect of the change in KCS speed on self-propulsion parameters was also studied. The Froude number increase caused an increase in thrust and torque coefficients and a decrease in the advance coefficient. The pitch ratio, corresponding to the maximum open-water propeller efficiency value, differed depending on ship speed. This

indicates that an optimum propeller pitch must be identified to increase efficiency. Future studies are planned to include full size CFD simulations to visualize flow and give a better physical insight into the results.

## ACKNOWLEDGEMENTS

This project is supported by Scientific and Technological Research Council of Turkey (TUBITAK), Project ID: 218M372.

## Conflict of interest

The author(s) declared no potential conflicts of interest with respect to the research, authorship, and/or publication of this article.

## NOMENCLATURE

$A_E / A_0$	Blade area ratio
B	Breadth
$C_B$	Block coefficient
$C_F$	Frictional resistance coefficient
$C_T$	Total resistance coefficient
$C_V$	Viscous resistance coefficient
$C_W$	Wave resistance coefficient
D	Propeller diameter
Fr	Froude number
$g_0, g_1, g_2$	Coefficients of K_Q
J	Advance coefficient
k	Ship form factor
$k_0, k_1, k_2$	Coefficients of K_T
$K_T$	Thrust coefficient
K_Q	Torque coefficient
$L, L_{pp}, L_{WL}$	Various forms of ship length
n	Propeller rotation rate
P/D	Propeller pitch ratio
Q	Propeller torque
$R_T$	Ship total resistance
S	Ship wetted surface area
t	Thrust deduction factor
T	Propeller thrust (in Newtons)
$T_H$	Ship draft (in meters)
V	Ship velocity
w	Wake fraction
Z	Number of blades
$\eta_0$	Open-water propeller efficiency
$\lambda$	Scale model
$\rho$	Water density

## ABBREVIATIONS

BEM	Boundary Element Methods
CFD	Computational Fluid Dynamics
CPP	Controllable Pitch Propeller
DTC	Duisburg Test Case
EFD	Experimental Fluid Dynamics
FPP	Fixed Pitch Propeller
ITTC	International Towing Tank Conference
JBC	Japanese Bulk Carrier
KCS	KRISO Container Ship
LCF	Longitudinal Center of Flotation
LDV	Laser Doppler Velocimetry
MARIN	Maritime Research Institute Netherlands
RANS	Reynolds-averaged Navier-Stokes
SFC	Skin Friction Correction
SPE	Self-Propulsion Estimation method
SMTL	Ship Model Testing Laboratory

## REFERENCES

- Bakica, A. et al., 2019. Accurate assessment of ship-propulsion characteristics using CFD. *Ocean Engineering*, 175, pp.149–162. Available at: <http://dx.doi.org/10.1016/j.oceaneng.2018.12.043>.
- Belhenniche, S.E. et al., 2016. Effect of geometric configurations on hydrodynamic performance assessment of a marine propeller. *Brodogradnja*, 67(4), pp.31–48. Available at: <http://dx.doi.org/10.21278/brod67403>.
- Benini, E., 2003. Multiobjective Design Optimization of B-Screw Series Propellers Using Evolutionary Algorithms. *Marine Technology and SNAME News*, 40(04), pp.229–238. Available at: <http://dx.doi.org/10.5957/mt1.2003.40.4.229>.
- Bernitsas, M. M., Ray, D., & Kinley, P., 1981. KT, KQ and efficiency curves for the Wageningen B-series propellers. University of Michigan.
- Birk, L., 2019. Fundamentals of Ship Hydrodynamics. Available at: <http://dx.doi.org/10.1002/9781119191575>.
- Caldas, A., Meis, M., & Sarasquete, A., 2010. CFD validation of different propeller ducts on Open Water condition. In 13th Numerical Towing Tank Symposium, Germany.
- Can, U., Delen, C., & Bal, S., 2020. Effective wake estimation of KCS hull at full-scale by GEOSIM method based on CFD. *Ocean Engineering*, 218, p.108052. Available at: <http://dx.doi.org/10.1016/j.oceaneng.2020.108052>.
- Carrica, P.M., Castro, A.M. & Stern, F., 2010. Self-propulsion computations using a speed controller and a discretized propeller with dynamic overset grids. *Journal of Marine Science and Technology*, 15(4), pp.316–330. Available at: <http://dx.doi.org/10.1007/s00773-010-0098-6>.
- Carrica, P.M., Kim, Y. & Martin, J.E., 2019. Near-surface self propulsion of a generic submarine in calm water and waves. *Ocean Engineering*, 183, pp.87–105. Available at: <http://dx.doi.org/10.1016/j.oceaneng.2019.04.082>.
- Castro, A.M., Carrica, P.M. & Stern, F., 2011. Full scale self-propulsion computations using discretized propeller for the KRISO container ship KCS. *Computers & Fluids*, 51(1), pp.35–47. Available at: <http://dx.doi.org/10.1016/j.compfluid.2011.07.005>.
- Dang, J. et al., 2012. Quasi-steady two-quadrant open water tests for the Wageningen propeller C-and D-series. In Proceedings of the Twenty-Ninth Symposium on Naval Hydrodynamics, Gothenburg, Sweden.
- Dang, J., Van den Boom, H. J. J., & Ligtelijn, J. T., 2013. The Wageningen C-and D-series propellers. In 12th International Conference on Fast Sea Transportation FAST.
- Delen, C., & Bal, S., (2015). Uncertainty analysis of resistance tests in Ata Nutku Ship model testing Laboratory of Istanbul Technical University. *Turkish Journal of Maritime and Marine Sciences*, 1(2), pp. 69-88.
- Moctar, O. el, Shigunov, V. & Zorn, T., 2012. Duisburg Test Case: Post-Panamax Container Ship for Benchmarking. *Ship Technology Research*, 59(3), pp.50–64. Available at: <http://dx.doi.org/10.1179/str.2012.59.3.004>.
- Epps, B.P., Stanway, M.J. & Kimball, R.W., 2009. OpenProp: An Open-source Design Tool for Propellers and Turbines. Day 2 Wed, September 16, 2009. Available at: <http://dx.doi.org/10.5957/pss-2009-09>.
- Farkas, A., Degiuli, N. & Martić, I., 2018. Assessment of hydrodynamic characteristics of a full-scale ship at different draughts. *Ocean Engineering*, 156, pp.135–152. Available at: <http://dx.doi.org/10.1016/j.oceaneng.2018.03.002>.
- Gaafary, M.M., El-Kilani, H.S. & Moustafa, M.M., 2011. Optimum design of B-series marine propellers. *Alexandria Engineering Journal*, 50(1), pp.13–18. Available at: <http://dx.doi.org/10.1016/j.aej.2011.01.001>.
- Gaggero, S., Villa, D. & Viviani, M., 2017. An extensive analysis of numerical ship self-propulsion prediction via a coupled BEM/RANS approach. *Applied Ocean Research*, 66, pp.55–78. Available at: <http://dx.doi.org/10.1016/j.apor.2017.05.005>.
- Gokce, M.K., Kinaci, O.K. & Alkan, A.D., 2018. Self-propulsion estimations for a bulk carrier. *Ships and Offshore Structures*, 14(7), pp.656–663. Available at: <http://dx.doi.org/10.1080/17445302.2018.1544108>.
- Heinke, H. J., 2011. Potsdam Propeller Test Case (PPTC). Cavitation Tests with the Model Propeller VP1304. Schiffbau-Versuchsanstalt, Potsdam, Report, p. 3753.
- IMO, 2013. Resolution MEPC.232(65). Interim guidelines for determining minimum propulsion. Power to maintain the manoeuvrability of ships in adverse conditions, Annex 16.
- ITTC, 2014a. Example for Uncertainty Analysis of Resistance Tests in Towing Tanks. 7.5-02-02-02.1. ITTC, Recommended Procedures and Guidelines ITTC, 11.
- ITTC, 2014b. Example for Uncertainty Analysis of Resistance Tests in Towing Tanks - 7.5-02-02-02.1. In International Towing Tank Conference.
- ITTC, 2014c. General Guideline for Uncertainty Analysis in Resistance Tests - 7.5-02-02-02. In International Towing Tank Conference.
- ITTC, 2017a. 1978 ITTC Performance Prediction Method – 7.5-02-03-01.4. Propulsion Committee of the 28th ITTC.
- ITTC, 2017b. Open Water Test – 7.5-02-03-02.1." Propulsion Committee of the 28th ITTC.
- ITTC, 2017c. Recommended Procedures and Guidelines – Ship Models -7.5-01-01-01. Resistance Committee of the 28th ITTC.
- ITTC, 2017d. Resistance Test -7.5-02-02-01. In Resistance Committee of the 28th ITTC, 1–14.
- Jasak, H. et al., 2019. CFD validation and grid sensitivity studies of full scale ship self propulsion. *International Journal of Naval Architecture and Ocean Engineering*, 11(1), pp.33–43. Available at: <http://dx.doi.org/10.1016/j.ijnaoe.2017.12.004>.
- Ji, M. et al., 2018. Design and Optimization of Control System for Controllable Pitch Propeller with Load Protection. 2018 IEEE International Conference on Mechatronics and Automation (ICMA). Available at: <http://dx.doi.org/10.1109/icma.2018.8484605>.

- Kim, W.J., Van, S.H. & Kim, D.H., 2001. Measurement of flows around modern commercial ship models. *Experiments in Fluids*, 31(5), pp.567–578. Available at: <http://dx.doi.org/10.1007/s003480100332>.
- Kinaci, O.K. et al., 2018. ON SELF-PROPULSION ASSESSMENT OF MARINE VEHICLES. *Brodogradnja*, 69(4), pp.29–51. Available at: <http://dx.doi.org/10.21278/brod69403>.
- Kinaci, O.K., Gokce, M.K. & Delen, C., 2020. Resistance experiments and self-propulsion estimations of Duisburg Test Case at 1/100 scale. *Ship Technology Research*, 67(2), pp.109–120. Available at: <http://dx.doi.org/10.1080/09377255.2020.1729454>.
- Makino, H. et al., 2017. Energy savings for ship propulsion in waves based on real-time optimal control of propeller pitch and electric propulsion. *Journal of Marine Science and Technology*, 22(3), pp.546–558. Available at: <http://dx.doi.org/10.1007/s00773-017-0434-1>.
- Martelli, M. et al., 2013. Controllable pitch propeller actuating mechanism, modelling and simulation. *Proceedings of the Institution of Mechanical Engineers, Part M: Journal of Engineering for the Maritime Environment*, 228(1), pp.29–43. Available at: <http://dx.doi.org/10.1177/1475090212468254>.
- Oosterveld, M.W.C. & van Oossanen, P., 1975. Further computer-analyzed data of the Wageningen B-screw series. *International Shipbuilding Progress*, 22(251), pp.251–262. Available at: <http://dx.doi.org/10.3233/isp-1975-2225102>.
- Sezen, S. et al., 2018. Investigation of self-propulsion of DARPA Suboff by RANS method. *Ocean Engineering*, 150, pp.258–271. Available at: <http://dx.doi.org/10.1016/j.oceaneng.2017.12.051>.
- Sezen, S. et al., 2021. An investigation of scale effects on the self-propulsion characteristics of a submarine. *Applied Ocean Research*, 113, p.102728. Available at: <http://dx.doi.org/10.1016/j.apor.2021.102728>.
- Song, S., Demirel, Y.K. & Atlar, M., 2020. Penalty of hull and propeller fouling on ship self-propulsion performance. *Applied Ocean Research*, 94, p.102006. Available at: <http://dx.doi.org/10.1016/j.apor.2019.102006>.
- Tadros, M., Ventura, M. & Guedes Soares, C., 2019. Optimum design of a container ship's propeller from Wageningen B-series at the minimum BSFC. *Sustainable Development and Innovations in Marine Technologies*, pp.269–276. Available at: <http://dx.doi.org/10.1201/9780367810085-35>.
- Tadros, M., Ventura, M. & Guedes Soares, C., 2020. A nonlinear optimization tool to simulate a marine propulsion system for ship conceptual design. *Ocean Engineering*, 210, p.107417. Available at: <http://dx.doi.org/10.1016/j.oceaneng.2020.107417>.
- Tadros, M. et al., 2021. Coupled Engine-Propeller Selection Procedure to Minimize Fuel Consumption at a Specified Speed. *Journal of Marine Science and Engineering*, 9(1), p.59. Available at: <http://dx.doi.org/10.3390/jmse9010059>.
- Ukon, Y., Kurobe, Y. & Kudo, T., 1989. Measurement of Pressure Distribution on a Conventional and a Highly Skewed Propeller Model. *Journal of the Society of Naval Architects of Japan*, 1989(165), pp.83–94. Available at: <http://dx.doi.org/10.2534/jjasnaoe1968.1989.83>.
- Van, S. H. et al., 1998. Experimental Investigation of the Flow Characteristics around Practical Hull Forms. In *3rd Osaka Colloquium on Advanced CFD Applications to Ship Flow and Hull Form Design*.
- Villa, D. et al., 2019. An efficient and robust approach to predict ship self-propulsion coefficients. *Applied Ocean Research*, 92, p.101862. Available at: <http://dx.doi.org/10.1016/j.apor.2019.101862>.
- Xiong, Y., Wang, Z. & Qi, W., 2013. Numerical study on the influence of boss cap fins on efficiency of controllable-pitch propeller. *Journal of Marine Science and Application*, 12(1), pp.13–20. Available at: <http://dx.doi.org/10.1007/s11804-013-1166-9>.
- Yuan, Z.-M. et al., 2018. Side wall effects on ship model testing in a towing tank. *Ocean Engineering*, 147, pp.447–457. Available at: <http://dx.doi.org/10.1016/j.oceaneng.2017.10.042>.